Intermediate States of Subfragment 1 and Actosubfragment 1 ATPase: Reevaluation of the Mechanism†

Kenneth A. Johnson and Edwin W. Taylor*

ABSTRACT: The kinetics of the increase in protein fluorescence following the addition of ATP to subfragment-1 (SF-1) and acto-SF-1 have been reinvestigated. The concentration dependence of the rate obtained with SF-1 did not fit a hyperbola and at high ATP concentration, approximately 40% of the signal amplitude was lost due to a fast phase at the beginning of the transient (20 °C). At lower temperature (≤10 °C) the fluorescence transient was biphasic, with a fast phase observed at high ATP concentration. These results indicate that there are two steps in the SF-1 pathway in which there is a change in protein fluorescence. Measurements of ATP binding and hydrolysis by chemical quench-flow methods indicate that the rate of ATP binding is correlated with the fast fluorescence step and hydrolysis is correlated with the slow fluorescence change. The SF-1 mechanism can thus be described as:

$$M + ATP \overset{1}{\rightleftharpoons} M{\cdot}ATP \overset{2}{\rightleftharpoons} M{\cdot}ATP^* \overset{3}{\rightleftharpoons} M{\cdot}ADP\,P_i{}^{**} \overset{slow}{\rightleftharpoons} M + ADP + P_i$$

where M represents SF-1 and states of enhanced fluorescence are given by M* (16%) and M** (36% enhancement, relative to SF-1). Step 1 is a rapid equilibrium with $K_1 \sim 10^3\ M^{-1}$. Tight binding of ATP occurs in step 2 and the loss of signal amplitude requires $k_2 \gtrsim 1500$–$2000\ s^{-1}$. The maximum observed fluorescence rate defines the rate of hydrolysis, $k_3 + k_{-3} = 125\ s^{-1}$ (20 °C, 0.1 M KCl, pH 7.0). The steps in the mechanism correspond to the Bagshaw–Trentham scheme, with the important difference that the assignment of rate constants is altered. Formation of the acto-SF-1 complex gave a fluorescence enhancement of approximately 14% relative to SF-1. Dissociation of acto-SF-1 by ATP produced a 20–22% enhancement in fluorescence. There was no detectable fluorescence change during dissociation as evidenced by a lag in the fluorescence transient which corresponded to the kinetics of dissociation. The fluorescence change occurred at the same maximum rate as for SF-1 but there was no loss in signal amplitude at high ATP concentration. The kinetics of the fluorescence change corresponded to the rate of ATP hydrolysis, whereas tight ATP binding occurred at a much faster rate in approximate agreement with the rate of dissociation. Thus the fluorescence change in the acto-SF-1 pathway corresponds to step 3 in the SF-1 mechanism. The complete scheme can be described as follows:

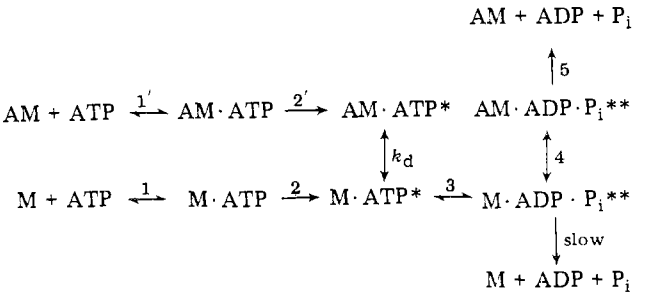

where AM represents acto-SF-1. The tight binding step in the SF-1 pathway (k_2) is sufficiently fast so that a similar step (k_2') in the acto-SF-1 pathway could precede dissociation but the AM·ATP* intermediate has not been detected. Following hydrolysis on the free SF-1, actin recombines with M·ADP·P_i** or possibly with a second SF-1 product intermediate as proposed by Chock et al. (1976) and the fluorescence returns to the original AM level with product release.

The mechanism of the subfragment 1 (SF-1)[1] ATPase has been investigated in several laboratories (Lymn & Taylor, 1970; Taylor et al., 1970; Bagshaw et al., 1974; Bagshaw & Trentham, 1974; Chock & Eisenberg, 1974; Koretz & Taylor, 1975) employing enhancement of tryptophan fluorescence (Werber et al., 1972), proton release, and direct measurement of phosphate production. A scheme was proposed by Bagshaw and Trentham (1974) which accounted for much of the evidence and represented a significant step in understanding the mechanism:

$$M + ATP \overset{1}{\rightleftharpoons} M{\cdot}ATP \overset{2}{\rightleftharpoons} M{\cdot}ATP^* \overset{3}{\rightleftharpoons} M{\cdot}Pr^{**} \overset{slow}{\rightleftharpoons} M + Pr \quad (1)$$

where M refers to a myosin head or SF-1, Pr is the product of hydrolysis, and asterisks indicate enhancement of tryptophan fluorescence. Since hydrolysis is followed by a slow rate-limiting step and we are concerned only with the steps up to hydrolysis, the scheme can be treated as a three-step reaction.

The proposed mechanism was based essentially on the findings that the fluorescence signal at any ATP concentration showed no lag and could be fitted satisfactorily by a single exponential term. The apparent rate constant increased with ATP concentration to a maximum value of about $400\ s^{-1}$ (pH 8, 20 °C, 0.1 M KCl) and the concentration dependence of the rate fitted a hyperbola. It should be noted that these observations are also consistent with a two-step mechanism in which the initial step is a rapid equilibrium and the fluorescence

† From the Department of Biophysics and Theoretical Biology, The University of Chicago, Chicago, Illinois 60637. *Received February 8, 1978.* This work was supported by a Grant from the National Institutes of Health (HL20592) and by the Muscular Dystrophy Association of America.

[1] Abbreviations used: SF-1, subfragment 1; HMM, heavy meromyosin; ATP, adenosine 5′-triphosphate; ATPase, adenosine triphosphatase; AMP PNP, β,γ-imidoadenosine 5′-triphosphate; ADP, adenosine 5′-diphosphate; Tris, 2-amino-2-hydroxymethyl-1,3-propanediol; Mes, 4-morpholineethanesulfonic acid.

0006-2960/78/0417-3432$01.00/0

transition occurs in the second step. The fit to a hyperbola then defines the association constant for the first step and the maximum rate defines the rate of the fluorescence transition. However, the scheme has two fluorescence transitions and, although the relative amplitudes were not determined, it was suggested that the increase in fluorescence for each of the transitions (steps 2 and 3) was approximately equal, that is, 10% and 20% enhancements for states M·ATP* and M·Pr**, respectively, relative to M (for papain SF-1). In part, this assignment was inferred by noting that a nonhydrolized nucleotide (AMPPNP) gave a 10% enhancement. In addition, ADP showed similar kinetics and gave the same maximum rate as ATP, although the amplitude of the fluorescence enhancement was only 6%. It was thus inferred that it was step 2 which was common to both the ATP and ADP pathways and the maximum rate of the fluorescence signal determined k_2. It was further proposed that the larger signal observed with ATP resulted from a transition that occurred only with hydrolysis (step 3).

A three-step mechanism in which the first step is a rapid equilibrium would be expected to fit two exponential terms rather than one. To account for this discrepancy it was suggested that k_3 was much greater than k_2 so that the second fluorescence step would be rate limited by k_2 and only a single rate process would be observed. A similar proposal was made by Koretz & Taylor (1975) based on H^+ and phosphate measurements.

The Bagshaw–Trentham scheme provided a logical synthesis of the available evidence but further studies at various pHs and temperatures have raised difficulties. At pH 7 and 3 °C the fluorescence rate was slightly faster than hydrolysis but quenching with excess unlabeled ATP showed the presence of an appreciable fraction of tightly bound ATP during the transient (Sleep & Taylor, 1976; Taylor, 1977). If $k_2 \ll k_3$ we would expect ATP to be converted to products as soon as it is tightly bound in the M·ATP* state. To account for the presence of M·ATP* during the transient, k_2 and k_3 would have to be comparable in magnitude and the fluorescence signal would be biphasic if steps 2 and 3 gave the same fluorescence enhancement.

Extension of the scheme to actomyosin also led to an apparent contradiction (Sleep & Taylor, 1976). At high ATP concentration, acto-SF-1 was shown to dissociate at a very high rate ($>700\ s^{-1}$) with no net change in fluorescence; dissociation was followed by a fluorescence signal of the same rate and the same amplitude as for SF-1. The maximum rate of hydrolysis was also unchanged. If the first dissociated state is M·ATP*, the fluorescence signal after dissociation should correspond to the transition M·ATP* to M·Pr** (step 3). Thus, according to the Bagshaw–Trentham scheme at a very high ATP concentration the rate of the fluorescence signal and of the hydrolysis step should have been much larger for acto-SF-1 than for SF-1, while the amplitude of the fluorescence signal should have been half as large. It was concluded that, if the Bagshaw–Trentham scheme was to be retained, it was necessary to suppose that acto-SF-1 dissociates into a state, symbolized by $M{\cdot}ATP^+$, which was not on the myosin pathway. The suggestion was rather forced since it did not explain why the fluorescence and hydrolysis rates should be the same in both pathways. Chock et al. (1976) obtained similar results for the rate of fluorescence enhancement, but reported the amplitude to be only half as large for acto-SF-1. They suggested that their results were consistent with the Bagshaw–Trentham scheme. While this interpretation accounted for the lower amplitude of the signal at high ATP concentrations, it also required k_2 to be equal to k_3. If this were the case, the fluorescence signal for SF-1 would be biphasic contrary to the observations of Bagshaw et al. (1974), who assumed that k_3 was much greater than k_2 in order to avoid this contradiction. An additional problem is that approximately half of the expected fluorescence signal was missing in the experiments of Chock et al. It was proposed that a fluorescence change accompanied dissociation and was too fast to observe at high ATP concentrations or possibly that a further transition might cancel out the signal expected for the formation of M·ATP*. The studies of Sleep & Taylor which covered a wide range of ATP concentrations ruled out the first explanation. Some evidence for an increase in fluorescence on formation of the acto-SF-1 complex was obtained but was considered to be inconclusive because of possible light scattering artifacts.

Neither the proposal of Sleep & Taylor nor the interpretation of Chock et al. is a completely satisfactory explanation of the experimental results and the difficulty appeared to arise from the attempt to fit the acto-SF-1 data into the requirements of the Bagshaw–Trentham scheme. The present series of experiments was undertaken to reexamine the evidence for this scheme and to locate the source of the discrepancy in the fluorescence amplitudes reported by the two laboratories. Our data indicate that the fluorescence signal obtained with SF-1 deviated from a single rate process, that the concentration dependence of the apparent rate did not fit a hyperbola, and that the amplitude of the observed signal decreased at high ATP concentrations. This evidence is consistent with the mechanism proposed by Bagshaw & Trentham in that there are two fluorescence transitions, but with the important difference that $k_2 \gg k_3$. The maximum rate at high ATP concentration measures k_3, the hydrolysis step, rather than k_2. This reassignment of the rate constants removes the contradictions in the acto-SF-1 scheme. In addition, the finding of a fluorescence enhancement on the formation of the acto-SF-1 complex, together with the observation that part of the fluorescence signal was lost in the reaction of ATP with SF-1, accounts for the "missing" fluorescence.

Materials and Methods

Preparation of Proteins. Myosin and actin were prepared from rabbit back and leg muscles by the methods of Perry (1955) and Spudich & Watt (1971), respectively. Heavy meromyosin (HMM) and subfragment 1 (SF-1) were prepared by chymotryptic digestion and were purified by DEAE-cellulose column chromatography for some experiments (Weeds & Taylor, 1975). The two species of SF-1 obtained in the column purification step were used for some of the kinetic experiments. To produce HMM, myosin was digested in 10 mM Tris, 10 mM Mes, pH 7.0, 0.6 M KCl, 4 mM $MgCl_2$, 1 mM ETDA with 0.05 mg/mL α-chymotrypsin (Sigma Chemical Co., St. Louis, Mo.) for 10 min at 25 °C. To produce SF-1, myosin was dialyzed from 0.6 M NaCl into 10 mM Tris, 10 mM Mes, pH 7.0, 0.12 M NaCl, 1 mM ETDA and digested with 0.5 mg/mL α-chymotrypsin for 20 min at 25 °C. In both cases, digestion was stopped by the addition of 0.1 mM phenylmethanesulfonyl fluoride (Sigma Chemical Co.). For some experiments SF-1 was prepared by digestion with papain by the method of Lowey et al. (1969) as modified by Margossian et al. (1975).

Protein concentrations in mg/mL were calculated from the following relationships: $[\text{myosin}] = (A_{280} - 1.5A_{320})/0.533$, $[\text{actin}] = (A_{290} - 1.34A_{320})/0.69$, $[\text{HMM}] = A_{280}/0.647$, $[\text{papain SF-1}] = A_{280}/0.78$, $[\text{chymotryptic SF-1}] = A_{280}/0.75$. The extinction coefficient for chymotryptic SF-1 is from a recent determination by Weeds & Pope (1976). A correction for light scattering by solutions of actin and myosin was based

upon the A_{320} as indicated. Molecular weights were assumed to be 1.0, 1.15, 3.4, and 4.9 × 10^5 g/mol for chymotryptic SF-1, papain SF-1, HMM, and myosin, respectively, and 42 500 g/mol for actin. The smaller molecular weight for chymotryptic SF-1 as compared with papain SF-1 was used since the chymotryptic SF-1 preparations lacked the P-light chains.

Fluorescence Measurements. Steady-state and equilibrium fluorescence measurements were made using a Perkin-Elmer MPF-4 fluorescence spectrophotometer. Samples were excited at 294 nm (5 nm half-width) and the emission spectra were scanned using a 2-nm half-width and with a 290-nm UV cut filter on the output. The temperature of the sample chamber was controlled using a circulating water bath.

Transient state fluorescence measurements were made using a stopped-flow instrument constructed in this laboratory. The path length of the cell is 2 mm. The incident beam from a mercury arc lamp was passed through a 294-nm interference filter. Fluorescence was measured at 90° to the incident beam using a 290-nm UV cut filter (Ealing Optics 26-4655) and a 330-nm interference filter. Transmitted beam intensity was measured with a photodiode and displayed on a digital voltmeter. Unless a change in turbidity occurred in the experiment, the fluorescence signal was divided by the transmitted beam intensity to reduce lamp fluctuations. Light scattering was recorded simultaneously at 90° to the incident beam using a 290-nm interference filter.

As described in the Results (see Figure 1) the percent fluorescence enhancement depended upon the wavelength of emission. Therefore, in order to compare results obtained in the stopped-flow apparatus with the emission spectra obtained in the fluorescence spectrophotometer, it was necessary to consider the band pass of the filters used to isolate the fluorescence signal in the stopped flow. Computation of the expected relative enhancement from the fluorescence emission spectra (Figure 1) was based upon a weighted average: $I_{av} = \Sigma T_\lambda I_\lambda / \Sigma T_\lambda$ where the weighting factor at each wavelength was the percent transmittance (T_λ) of the filters used in the stopped-flow apparatus. I_λ was the observed intensity at wavelength λ and the sum was taken from 310 nm to 370 nm.

For experiments measuring the fluorescence change upon acto-SF-1 association, a relatively small fluorescence change was observed in conjunction with a large light scattering change in the same direction. Therefore, it was necessary to determine whether the apparent fluorescence change was due to leakage of scattered 294 nm light through the fluorescence channel. Substitution of a 290-nm interference filter of the same percent transmission for the 330-nm filter showed that the change in intensity of scattered light at the exciting wavelengths which was transmitted by the 290 nm UV cut filter was ten times smaller than the "fluorescence" signal obtained in the association of actin with SF-1. A much smaller fraction of scattering intensity would pass the 330-nm filter; consequently a change in light scattering could make only a very small contribution to the change in fluorescence intensity. Also, the addition of a nonfluorescent scatterer (polystyrene latex spheres) at a concentration which gave a light-scattering signal comparable to acto-SF-1 led to a negligible increase in voltage in the fluorescence channel. Therefore the voltage change observed in the fluorescence channel upon acto-SF-1 association was a measure of a change in protein fluorescence.

Kinetic Analysis. Voltages from the fluorescence and light-scattering channels were stored vs. time in digital form in a PDP 11/10 computer and plotted using a Hewlett-Packard X-Y recorder. By recording the voltage used to offset the output from the photomultipliers and the gain settings used to amplify the signals, the plot on the X-Y recorder was converted to absolute voltages for each channel so that the size of signals could be precisely quantitated. A correction for the voltage obtained with buffer in the cell was negligible.

Data were fitted to a single exponential of the form $y = a \exp(-\lambda t) + b$ by a nonlinear least-squares method (Sleep & Taylor, 1976). In those cases where biphasic curves were observed, the fit was begun using points following the fast phase. Because of the small size of the fast phase, a fit to a double exponential was not feasible.

Chemical Quench-Flow. Measurement of a rapid transient phosphate production was performed using a chemical quench flow apparatus built in this laboratory and described previously (Taylor, 1977). SF-1 or acto-SF-1 was mixed with [γ-^{32}P]ATP and then passed through a lucite cylinder to a second mixer where the reaction was either stopped with 3 N PCA or quenched with an excess of unlabeled ATP.

The efficiency of mixing was investigated by attaching an optical cell just below the mixer and examining the change in cresol red absorption in a pH jump. A solution of 90 μM cresol red in 10 mM Tris-Mes, pH 6.5, was mixed with 100 mM Tris, pH 8.5, and the change in transmittance at 533 nm was recorded. There was a fivefold decrease in transmittance when these solutions were mixed yet no change was detectable as a transient immediately following mixing. Thus, within the limits of detectability mixing was 99% complete (0.05-V noise on a 5-V signal). The time between mixing and observation was determined to be 3 ms from the volume rate of flow and the volume between the mixer and the observation cell. Thus, the mixing was at least 99% complete within 3 ms.

Reaction times were varied by interchanging lucite cylinders of different lengths and by varying the drive pressure. Following the addition of unlabeled ATP in the quench experiment, the reaction was stopped within 1-2 s by manually adding 3 N PCA. Carrier phosphate (10^{-4} M) was added and protein precipitates were removed by centrifugation. A 0.25-mL aliquot of the supernatant was counted in 10 mL of 0.1 N HCl to determine total radioactivity. A second aliquot of 2 mL was filtered using a charcoal-Celite column (2 mL of a 1:1 charcoal-Celite mixture) to adsorb ATP; the column was washed with 8 mL of 0.1 N HCl and the filtrate was counted to determine [^{32}P]phosphate. Radioactivities in each fraction were determined by the Cerenkov method using a Packard Tri-Carb scintillation counter. The zero time blank was generally 1% of the total radioactivity. With complete hydrolysis, 100% of the counts were recovered as phosphate.

The reactions under study have large temperature coefficients. During the experiments the temperature in the reservoir syringes and just adjacent to the mixing chambers of the stop-flow and quench-flow machines were measured by means of thermocouple probes (Bailey Instruments, Saddle Brook, N.J.). At the end of the experiment, the temperature within the reaction chamber was measured. The temperature error in comparing stop-flow and quench-flow measurements was less than 1 °C.

Results

The Amplitude of the Fluorescence Enhancement. We initially characterized the amplitude of the fluorescence enhancement following the addition of ATP to SF-1 and to acto-SF-1 by steady-state measurements. The relative magnitudes of the fluorescence changes for these two species are important in relating the acto-SF-1 ATPase mechanism to the SF-1 pathway. To establish the relative fluorescence of SF-1

and acto-SF-1, we investigated whether there was a change in fluorescence occurring in the formation of the acto-SF-1 complex and compared the amplitude of the fluorescence change following the addition of ATP to each species.

The fluorescence emission spectra were determined for solutions of actin, SF-1 and acto-SF-1 prepared at the same molar site concentration in the presence and absence of excess ATP. In order to obtain the most accurate measurements, solutions of SF-1 and actin were mixed 1:1 to obtain acto-SF-1 and the same SF-1 and actin solutions were diluted 1:1 with buffer for comparison. The ATP-induced enhancement in fluorescence was determined after the addition of a small aliquot of an ATP stock solution such that the dilution of the protein was negligible (0.5%).

The results of one experiment are shown in Figure 1. The left figure shows the emission spectra of actin (A), SF-1 (M), and acto-SF-1 (AM), and the right figure shows the spectra of the same SF-1 and acto-SF-1 solutions following the addition of ATP. There was no change in the spectra following the addition of ATP to the actin (not shown). Difference spectra are indicated by dashed lines.

The difference spectrum in the left figure indicates a fluorescence enhancement for the acto-SF-1 association reaction. The difference spectra in the right figure define the fluorescence enhancement for SF-1 (ΔM) and for acto-SF-1 (ΔAM), following the addition of ATP. The fluorescence change observed for SF-1 was larger than for acto-SF-1 at all wavelengths. The difference between the enhancement observed for SF-1 and acto-SF-1 ($\Delta M - \Delta AM$) was equal to the increase in fluorescence observed on the formation of the acto-SF-1 complex (left figure). Thus there was an increase in fluorescence on the association of actin with SF-1, but following the addition of ATP both SF-1 and acto-SF-1 yielded the same final state of fluorescence enhancement.

We further analyzed the change in fluorescence for acto-SF-1 association using the stopped-flow apparatus to directly measure the amplitude of the fluorescence transient following the mixing of SF-1 with actin. Actin (4.4 μM) and SF-1 (4 μM) were mixed in the stopped-flow and changes in fluorescence and light scattering were recorded simultaneously. A fluorescence enhancement of 12% relative to SF-1 was observed. As described in Materials and Methods, the observed fluorescence increase was not a result of the light-scattering change affecting the fluorescence channel. Within the limits of error, the fluorescence and light-scattering signals gave the same rate when fitted to a second-order program. Although the question of whether the fluorescence change occurred as a first-order transition following association has not been properly examined, these data provide direct evidence for a fluorescence increase on the association of SF-1 with actin.

The fluorescence enhancement of acto-SF-1 was also measured by dissociating the complex with 1 mM pyrophosphate. Acto-SF-1 was completely dissociated in the presence of 1 mM pyrophosphate as measured by the size of the light-scattering change. An 8% decrease in fluorescence was observed which occurred at the same rate as dissociation. Since the binding of pyrophosphate to SF-1 gave a 1–2% increase in fluorescence, these experiments indicate a 9–10% enhancement of fluorescence in the acto-SF-1 complex in approximate agreement with the above measurements.

To quantitatively compare these results with those obtained in the fluorescence spectrophotometer, it is necessary to take into account the transmission spectrum of the filter used to isolate the fluorescence signal in the stopped-flow apparatus. Since there was a blue shift in the emission maximum relative to the SF-1 peak (Figure 1), the relative enhancement de-

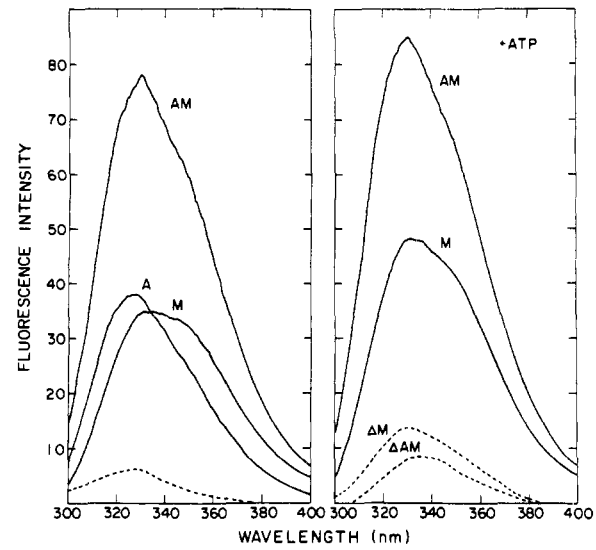

FIGURE 1: Fluorescence emission spectra. The emission spectra were recorded as described in Materials and Methods for 1.8 μM SF-1, 1.9 μM actin, 1.8 μM acto-SF-1 (left figure) and the same SF-1 and acto-SF-1 solutions with 500 μM ATP added (right figure). The dilution of the SF-1 and acto-SF-1 solutions by the addition of ATP (10 μL of 100 mM ATP stock added to 2.0 mL) was negligible. Difference spectra are shown by dashed curves (see text). Conditions: 20 °C, 0.1 M KCl, 4 mM $MgCl_2$, 10 mM Tris-Mes, pH 7.

pended upon the wavelength. For example, at 330 nm there was an 18% increase relative to SF-1, whereas at 340 nm the increase was only 10%. The fluorescence change expected in the stopped-flow was calculated from a weighted average of the fluorescence spectra. The contribution of the intensity at each wavelength to the sum was weighted by the interference filter transmittance at that wavelength (see Materials and Methods). The weighted averages of the intensities of actin, SF-1, and acto-SF-1 predict that a 14% enhancement would be observed for the acto-SF-1 association reaction in the stopped-flow. Similar analyses of the SF-1 and acto-SF-1 spectra in the presence of ATP predict a relative enhancement of 36% and 21% for the reaction of ATP with SF-1 and acto-SF-1, respectively. Stopped-flow measurements gave enhancements of 36–38% and 20–24%, respectively. The overall enhancement for acto-SF-1 in the presence of ATP (14% plus 21%) was the same as the enhancement observed for SF-1 (36%), so both species achieved the same final state.

The increase in fluorescence and the slight blue shift following the addition of ATP to SF-1 agree with the original description by Werber et al. (1972). However, the amplitude of the change was approximately twice that previously reported. We therefore investigated the methods used to prepare the proteins in an attempt to resolve this possible discrepancy.

The previous studies were performed using either HMM or SF-1 prepared by papain digestion, while the proteins used in the current work were prepared by the digestion of myosin with α-chymotrypsin. In order to determine whether the digestion procedure directly affected the size of the fluorescence change, we compared the signals obtained with papain SF-1, chymotryptic SF-1, HMM, and myosin. By preparing these four proteins at the same site concentration, the size of the fluorescence change was compared in terms of the absolute magnitude of the change as well as the percentage enhancement. Since the purity and the activity of the protein affect the size of the fluorescence change, two methods were used to prepare the proteins in hopes of obtaining a valid comparison. To prepare one set of proteins, we first purified myosin by a batch

TABLE I: The Magnitude of the Fluorescence Change.[a]

myosin subfragment	digestion enzyme	set A			set B		
		I_0	ΔI	%	I_0	ΔI	%
SF-1	α-chymotrypsin	28.0	10.0	35.8			
SF-1 (A1)	α-chymotrypsin				27.7	11.3	40.8
SF-1 (A2)	α-chymotrypsin				28.0	10.3	36.6
SF-1	papain	40.3	10.4	25.8	41.0	10.4	25.4
HMM	α-chymotrypsin	50.9	10.0	19.7	51.3	11.0	21.5
myosin		82.8	9.1	11.0	80.1	10.4	13.0

[a] Changes in fluorescence for various proteins, prepared by digestion of myosin with either α-chymotrypsin or papain, were determined by steady-state fluorometry following the addition of 100 μM ATP to 5 μM protein (see Materials and Methods). Figures in the columns headed by I_0, ΔI, and % give the initial intensity of fluorescence for each protein per ATP binding site, the change upon the addition of ATP, and the percent increase at 330 nm. Conditions: 20 °C, 10 mM Tris, 10 mM Mes, 0.1 M KCl, 4 mM $MgCl_2$, pH 7.0, except that the buffer solutions for myosin contained 0.5 M KCl. For set A, myosin was purified by a DEAE-Sephadex batch procedure and the proteins prepared by the digestion of this myosin were purified only by ammonium sulfate fractionation. For set B, myosin was column purified and the subfragments derived from it were individually column purified following digestion and ammonium sulfate fractionation (see Materials and Methods).

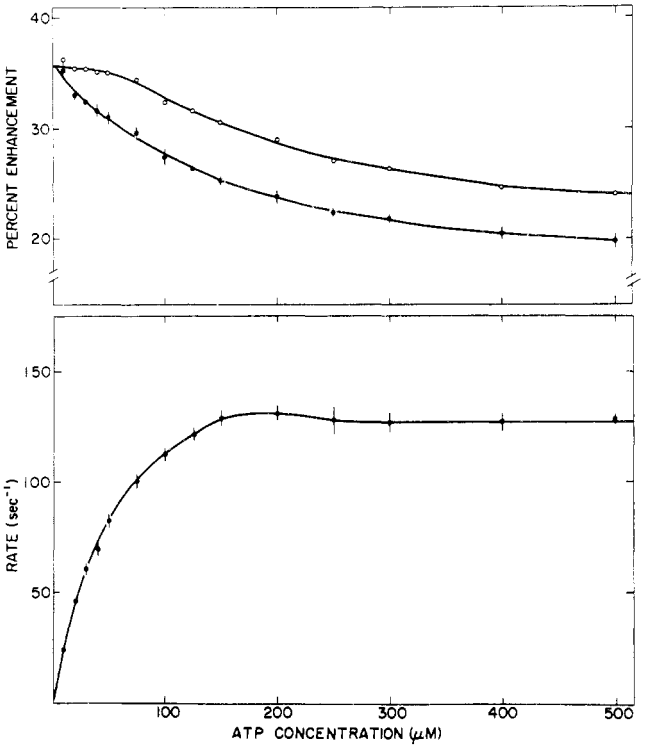

FIGURE 2: Rate of the fluorescence transient. The rates of the fluorescence transient following the mixing of ATP with SF-1 were obtained as the best fit to a single exponential and are plotted vs. the final ATP concentration in the lower graph. In the upper graph, the percent enhancement was calculated from the amplitude of the observed signal (●) and corrected (○) for expected loss of amplitude by the equation $A_{corr} = A_{obsd} \exp(kt)$ where t = dead time and k = the observed rate. Error bars denote the standard deviation of the mean of 3-4 traces. Conditions: 20 °C, 0.1 M KCl, 4 mM $MgCl_2$, 10 mM Tris-Mes, pH 7, 1.4 μM SF-1.

modification of the column method of Starr & Offer (1971) and then digested the myosin to produce SF-1 and HMM, which were then purified only by ammonium sulfate fractionation. This procedure led to somewhat cleaner preparations of SF-1 and HMM than from conventionally purified myosin as judged by polyacrylamide gel electrophoresis and allowed direct comparison of all proteins prepared on the same day from the same myosin. In a second set, each protein was separately column purified by the method of Weeds & Taylor (1975) following digestion of myosin and a separate purification of myosin was performed by the method of Starr & Offer (1971). This second method produced purer proteins, but the extra time required for the column procedure introduced an additional variable into the comparisons.

Changes in fluorescence were measured in the stopped-flow apparatus by mixing the protein with a low concentration of ATP so as to avoid the loss of signal observed at high rates (see below) or by measuring the fluorescence of protein alone versus protein plus excess ATP using a fluorescence spectrophotometer as in Figure 1. Similar results were obtained using both instruments in terms of the percentage fluorescence change. The results obtained by steady state measurements are shown in Table I.

These measurements indicate that the percentage fluorescence change does depend on the type of preparation. However, the magnitude of the change in fluorescence per site for all six column purified proteins was 10.7 ± 0.5. This variation was not much larger than expected from the errors in extinction coefficients and molecular weights of the respective proteins. The variation in the percent enhancement was principally a function of differences in the starting level of fluorescence. The differences in the basal fluorescence levels for chymotryptic SF-1, papain SF-1, and HMM were attributable to differences in purity of the proteins and the retention or loss of the P-light chains. That is, comparison of these proteins by $NaDodSO_4$-polyacrylamide gel electrophoresis indicated that the chymotryptic SF-1 preparations were the most pure but lacked the P-light chains, whereas papain SF-1 and HMM retained the P-light chains. Since the amplitude of the fluorescence enhancement was the same for all species, it appears that the tryptophan residue of the P-light chain does not contribute to the change in fluorescence on ATP binding but does increase the basal level of fluorescence. In addition, the two SF-1 isozymes containing A1 and A2 light chains were almost equal in terms of the amplitude of the fluorescence change.

We conclude that the digestion did not alter the fluorescence enhancement except by decreasing the background fluorescence while the absolute amplitude of the change was the same for SF-1, HMM, and myosin. Because the larger percentage signal change allowed more accurate data to be obtained, experiments were performed using chymotryptic SF-1 unless otherwise stated.

Kinetics of the Fluorescence Transient. The rate and amplitude of the fluorescence transient following the mixing of SF-1 and ATP were determined as a function of ATP concentration to obtain the results shown in Figure 2. The ATP concentration dependence of the rate did not fit a hyperbola and the apparent maximum rate decreased slightly at high ATP concentration (lower figure). The amplitude of the observed signal (upper figure) decreased with increasing ATP concentration and continued to decrease after the maximum

rate had been attained. The amplitudes corrected for signal loss employing the measured dead time of the instrument and the observed rate constant are shown by the open circles in the figure. At low ATP concentrations (less than 50 μM) the corrected amplitude was constant, indicating that over this concentration range, the actual loss of signal was commensurate with the observed increase in rate. At higher ATP concentrations the corrected amplitudes still decreased with increasing ATP concentration. Measurements of the intensity of the transmitted beam during the experiment showed that absorption by ATP was negligible and could not account for the loss of signal.

The results shown in Figure 2 were obtained using column purified chymotryptic SF-1 (A1 light chain). Essentially identical results were obtained for SF-1 (A2) both in terms of the observed rates and the loss of signal. The apparent second-order rate constant was $2.4 \pm 0.2 \times 10^6$ M^{-1} s^{-1} and the maximum rate was 125 ± 10 s^{-1} for each species (20 °C, pH 7, 0.1 M KCl). For HMM, a similar signal loss was observed and the same maximum rate was attained although the apparent second-order rate constant was slightly lower (2×10^6 M^{-1} s^{-1}). Papain SF-1 gave the same loss of signal, although the observed rates were somewhat lower with a maximum rate of 100 s^{-1}. Myosin and chymotryptic SF-1 in 0.5 M KCl gave results identical with each other, but at this ionic strength the maximum rate extrapolated to 550 s^{-1}. Up to the highest measured rate at 2 mM ATP (350 s^{-1}) there was no signal loss other than that which was attributable to an instrument dead time of 1.5 ms. The ionic strength dependence of the rate will be described more fully below. At pH 8 (20 °C, 0.1 M KCl, 10 mM Tris, 4 mM $MgCl_2$) chymotryptic SF-1 exhibited loss of signal and the dependence of the rate on ATP concentration deviated from a hyperbola in a manner similar to the results described above at pH 7. Under these conditions a maximum rate of 240 ± 25 s^{-1} was obtained.

The loss of signal, beyond that which was expected from the dead time of the instrument and the measured rate, and the nonhyperbolic concentration dependence of the rate suggest that there are two fluorescence transitions following ATP binding. At high ATP concentration, the first transition in the pathway becomes too fast to measure and accordingly the loss of signal is a measure of the increase in rate of the first transition with increasing ATP concentration; the total signal loss at high ATP concentration is an approximate measure of the size of this transition and its maximum rate. The total extent of signal loss suggests that the first transition gave a 16% change and the second transition gave a further 20% change (36% overall). For at least 90 to 95% of the amplitude of the first transition to be lost, the rate must have been at least 1500 to 2000 s^{-1}.

The fluorescence transient should be described by two exponential terms and under some conditions should be noticeably biphasic. At 20 °C, the signals were fitted by a single exponential with no detectable deviation, but at 5 °C the fluorescence signals exhibited a lag at low ATP concentration and a fast phase at high ATP concentration as shown in Figure 3 (upper half). At this temperature, only a 30% enhancement in fluorescence was observed with a fast phase accounting for approximately 10% of the signal amplitude. At 1 mM ATP approximately half of the 10% signal was lost which is consistent with a rate of 300–400 s^{-1} for the fast phase at this temperature and ATP concentration. Although the signal could not be accurately fitted to a double exponential program, the slow phase gave a fit to a single exponential with a maximum rate of 20.0 ± 0.4 s^{-1} under these conditions. These traces also show that the final level of fluorescence enhancement was the same for low and high ATP concentrations. Thus the signal amplitude was lost from the beginning of the transient which rules out loss of signal by absorption of the incident beam by ATP. Double mixing experiments also showed that loss of signal was a rate effect rather than an instrument artefact. SF-1 was mixed with a low ATP concentration which gave a 35% signal increase. A second mixing with a high ATP concentration after 1 s gave no change in amplitude other than that arising from dilution.

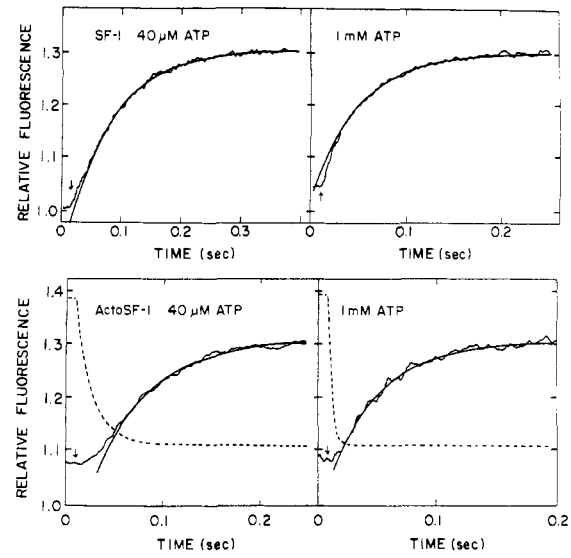

FIGURE 3: Kinetics of the fluorescence transient for SF-1 and acto-SF-1. Fluorescence was recorded as a function of time following the mixing of ATP with SF-1 (upper figures) and acto-SF-1 (lower figures). The fluorescence, relative to SF-1, is given by the jagged curve and the computer-fitted exponential is given by the smooth curve. The arrows designate the stop time. The dashed curves in the lower figures describe the kinetics of acto-SF-1 dissociation as measured by light scattering. Conditions: 5 °C, 0.1 M KCl, 10 mM Tris-Mes, pH 6.7, 4 mM $MgCl_2$, 1.1 μM SF-1, 1.1 μM acto-SF-1 (1.1 μM SF-1, 1.6 μM actin).

The loss of signal, the nonhyperbolic ATP concentration dependence of the rate observed at 20 °C, and the biphasic fluorescence transients observed at 5 °C provide evidence for two sequential fluorescence transitions following the addition of ATP to SF-1 (see Discussion).

Acto-SF-1 Kinetics. The kinetics of the fluorescence transient for acto-SF-1 were investigated under the same conditions as described above for SF-1 (5 °C, 0.1 M KCl, pH 7). Light scattering and fluorescence were recorded simultaneously. For the results shown in Figure 3 (lower figures), the fluorescence of the actin was subtracted from the observed signals to calculate the enhancement relative to SF-1. In contrast to the signals obtained with SF-1, the acto-SF-1 signals exhibited a lag at both low and high ATP concentration. The duration of the lag corresponded approximately to the kinetics of acto-SF-1 dissociation as measured by light scattering, indicating that the fluorescence change occurred after dissociation and that no measurable change occurred during dissociation. In addition the observed fluorescence amplitude was independent of ATP concentration and corresponded to the value obtained by static measurements at this temperature (20%) and thus there was no loss of signal. The acto-SF-1 traces began at a fluorescence level approximately 10% above SF-1 in keeping with our description of a fluorescence enhancement on the formation of the acto-SF-1 complex. The amplitudes of the signals observed for SF-1 at high ATP concentration approached the amplitude of the acto-SF-1 signal. Thus, the increase in fluorescence in forming the acto-SF-1 complex is approximately equal to the amplitude of the fast SF-1 signal

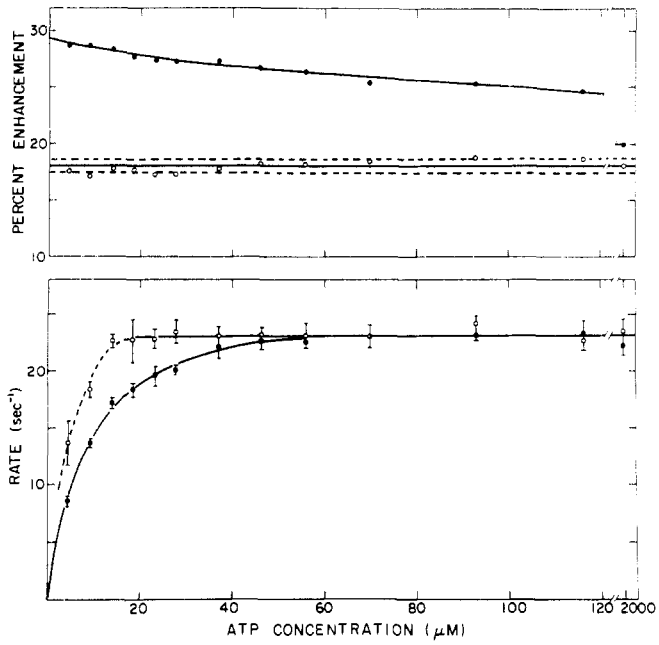

FIGURE 4: Rate and amplitude of fluorescence transient for SF-1 and acto-SF-1. The amplitude (upper figure) and the rate (lower figure) of the fluorescence transient are shown as a function of ATP concentration for SF-1 (●) and acto-SF-1 (○). In both cases the rate was obtained as a fit to a single exponential omitting the fast phase (SF-1) and the lag (acto-SF-1). In the portion of the acto-SF-1 curve described by the dashed line, the rate of dissociation was relatively slow and the lag was not well separated from the fluorescence increase (cf. Figure 3). Error bars denote the standard deviation of the mean of 3–4 traces. Conditions: 10 °C, 10 mM KCl, 10 mM Tris-Mes, pH 6.8, 4 mM $MgCl_2$, 2 μM SF-1, 2 μM acto-SF-1 (2 μM SF-1, 2.2 μM actin).

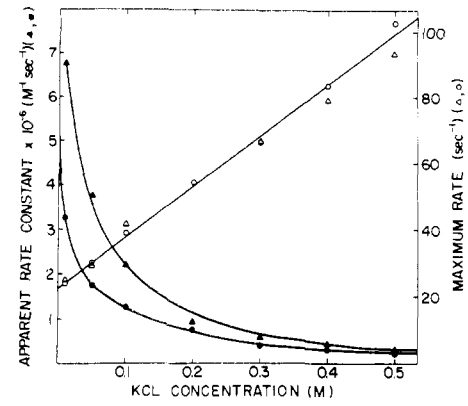

FIGURE 5: Ionic strength dependence. The kinetics of the fluorescence transient were measured following the mixing of ATP with SF-1 (●, ○) or acto-SF-1 (△) at various concentrations of KCl. The rate observed at 2 mM ATP gave the maximum rate (open symbols, right-hand scale). The rates observed at 10 μM ATP, divided by the ATP concentration, defined the apparent second-order rate constant (filled symbols, left-hand scale). The apparent second-order rate constant for acto-SF-1 dissociation (▲) was determined from the rate of the change in light scattering. The curves fitted to the apparent second-order rate constants (●, ▲) were calculated from the Debye-Hückel limiting law. Conditions: 10 °C, 10 mM Tris-Mes, pH 6.8, 4 mM $MgCl_2$, 2 μM SF-1, 2 μM acto-SF-1.

which is lost at high ATP concentration as described above (Figure 2).

These results suggest that only the slower of the SF-1 fluorescence transitions is observed with acto-SF-1. Thus the maximum rate should be the same for acto-SF-1 and SF-1. In addition, the signal amplitude for SF-1 at high ATP concentration should approach the acto-SF-1 amplitude as the fast SF-1 transition is lost. In order to further investigate the relationship of the SF-1 and acto-SF-1 signals, we have analyzed the concentration dependence of the rates and amplitudes obtained with both species at various temperatures and ionic strengths. The results reported below at 10 °C are representative of similar data at 5 and 20 °C.

The ATP concentration dependence of the rate and amplitude at 10 mM KCl and 10 °C is shown in Figure 4. These conditions were selected for study since they are optimal for comparison of the fluorescence transitions with the hydrolysis step which will be described in a later section (Kinetics of the Phosphate Burst). The concentration dependence of the rate (lower figure) deviated from a hyperbola for both acto-SF-1 and SF-1. For acto-SF-1 the deviation was more marked and the apparent second-order rate constant, k_a, defined by the initial slope, was greater than for SF-1. These results suggest that the initial rate of binding ATP to acto-SF-1 was slightly faster than the initial rate of binding to SF-1 (see Discussion). At ATP concentrations greater than 50 μM, the SF-1 signals were biphasic and were fitted to a single exponential omitting the first 10% of the trace as described in Figure 3; thus, the observed rates were a measure of the slow fluorescence step. As shown in Figure 4, the maximum rates obtained for SF-1 and acto-SF-1 were identical.

The amplitude data for SF-1 were obtained from the total observable signal including the fast phase to obtain the results given in the upper figure. The amplitudes of the acto-SF-1 signals were independent of ATP concentration within the limits of error; the dashed lines give the standard deviation of the mean. The amplitudes observed for SF-1 decreased with increasing ATP concentration, although the decrease in signal amplitude occurred over a higher range of ATP concentrations than was observed at 20 °C, 0.1 M KCl (Figure 2). This difference probably reflects the slower rate of the first fluorescence transition at this temperature and ionic strength. The results described here and those obtained at 20 °C, 0.1 M KCl, indicate that the amplitude and rate of the fluorescence transient observed for acto-SF-1 correspond to the second, slow step observed with SF-1.

Ionic Strength Dependence. To further compare the acto-SF-1 and SF-1 kinetics, the ionic strength dependence of the maximum fluorescence rate and the apparent second-order rate constant were determined. The maximum rate of the fluorescence change was determined at 2 mM ATP and the experiments at 4 mM ATP confirmed that the maximum rate had been attained. The apparent second-order rate constant was determined from the initial slope of rate vs. ATP concentration from the rates determined at 5 μM and 10 μM ATP. The results of these measurements are shown in Figure 5.

The apparent second-order rate constant of the SF-1 fluorescence transient decreased from 3.2 to 0.25 × 10^6 M^{-1} s^{-1} with increasing KCl concentration. The curve drawn through the points was derived from a straight line fit to a plot of ln k_a vs. the square root of the ionic strength. These data thus fit the Debye-Hückel limiting law with a charge product, $Z_A Z_B = -1.9$ which suggests that the initial association of ATP at the enzymic site involves some charge neutralization. A similar ionic strength dependence was observed for the rate of acto-SF-1 dissociation as measured by light scattering. Analysis by the Debye-Hückel limiting law suggests a charge product of $Z_A Z_B = -2.4$ for the initial association of ATP with acto-SF-1.

A large and nearly linear increase of the maximum fluorescence rate with increasing ionic strength was observed for both SF-1 and acto-SF-1. The agreement in the maximum rates observed for SF-1 and acto-SF-1 over this range of ionic strength supports the conclusion that the fluorescence transient

is a function of the same reaction for both enzyme forms. However, the basis for the linear increase in maximum rate with ionic strength cannot be easily explained. The amplitude of the fluorescence transient also increased by approximately 5% with increasing KCl concentration which suggests that the size of the phosphate burst may also depend upon ionic strength (see Discussion).

Essentially identical results were obtained using papain SF-1 and HMM and a similar dependence on ionic strength was observed at 20 °C.

Kinetics of the Phosphate Burst. The experiments described above indicate that there are two ATP induced fluorescence transitions for SF-1 and one for acto-SF-1. Therefore we investigated the transient kinetics of ATP hydrolysis by the chemical quench-flow method in order to determine which steps in the hydrolysis mechanism corresponded to the fluorescence transitions. The ATP concentration dependence of the fluorescence rate and amplitude for SF-1 and acto-SF-1 under the conditions used to analyze the phosphate burst (10 mM KCl, 10 °C) were described above (Figure 4). These conditions were chosen because the maximum fluorescence rate was attained at a moderately low ATP concentration and was sufficiently slow to allow reasonably accurate measurements of the phosphate burst by chemical quench-flow. The kinetics of the phosphate burst were determined at several ATP concentrations. We report below the results obtained at 75 μM, a concentration just above the plateau in rate.

The kinetics of the phosphate burst were determined by mixing [γ-^{32}P]ATP with SF-1 or acto-SF-1 and stopping the reaction at varying times with perchloric acid, then analyzing for [^{32}P]phosphate production as described previously (Taylor, 1977). In addition, the formation of a nondissociable ATP-SF-1 complex was measured by quenching the reaction at given times with excess unlabeled ATP to exchange off reversibly bound, labeled ATP and then stopping the reaction within 1–2 s by the addition of 1 volume of 3 N perchloric acid and analyzing for [^{32}P]phosphate. A parallel sample quenched with excess unlabeled ATP was incubated for 90 s before stopping the reaction with acid so as to allow all of the tightly bound ATP to be recovered as [^{32}P]phosphate. Both the 1–2 and 90 s incubations gave the same rate of formation of tightly bound ATP. The shorter incubation allowed the equilibration of ATP and ADP·P_i on the enzyme with no appreciable product release. The longer incubation (5 half-lives of the steady-state rate of product release) showed that 1.0 ± 0.05 ATP was bound per enzyme site. Typical results are shown in Figure 6. The phosphate data were scaled to the fluorescence traces obtained for SF-1 and acto-SF-1. The phosphate burst of 0.55 ± 0.05 in each case is most probably a measure of the equilibrium constant for hydrolysis (see Discussion) and is much less than unity due to the low temperature and ionic strength.

In the experiment with acto-SF-1 (lower figure), the kinetics of phosphate production corresponded closely to the kinetics of the fluorescence transition. The rate of tight ATP binding was faster than the phosphate rate and corresponded approximately to the rate of acto-SF-1 dissociation as measured by light scattering (dashed line). Thus, for acto-SF-1 the fluorescence change occurs during hydrolysis and there is apparently no net fluorescence signal associated with the tight ATP binding step. The data indicate that the first dissociated state in the acto-SF-1 pathway is an ATP·SF-1 complex with ATP irreversibly bound.

In the case of SF-1 (upper figure), the rate of phosphate production appeared somewhat slower than the fluorescence change and was much slower than the tight ATP binding reaction. The fluorescence transient was biphasic under these

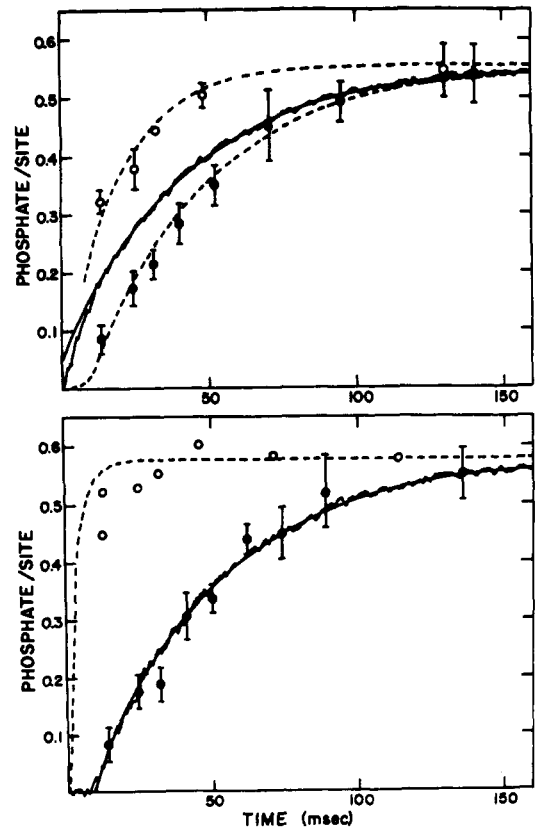

FIGURE 6: Time dependence of the phosphate burst. SF-1 or acto-SF-1 (10 μM final concentrations) was mixed with [γ-^{32}P]ATP (75 μM final) and at the times indicated either stopped with 1.3 N PCA (●) or quenched with 1.8 mM ATP and then stopped 1–2 s later with 1.3 N PCA (○), as described in Materials and Methods. The burst (0.55 mol of phosphate/site in each case) was scaled to fit the fluorescence trace given by the jagged line and smooth curve as described for Figure 3. The dashed line in the acto-SF-1 figure (lower) shows the kinetics of light scattering change for acto-SF-1 dissociation. The dashed lines in the SF-1 figure (upper) show a single exponential fit to the phosphate data. SF-1 rates: fluorescence, 22.9 ± 0.4 s^{-1}; phosphate, 24 ± 3 s^{-1}. Acto-SF-1 rates: fluorescence, 22.9 ± 1.1 s^{-1}; phosphate, 23 ± 3 s^{-1}; light scattering, 300 s^{-1}. Conditions: 10 °C, 10 mM Tris, 10 mM Mes, 10 mM KCl, 4 mM $MgCl_2$, pH 6.8.

conditions. The rate of the observed fast fluorescence transition approximately corresponded to the rate of tight ATP binding and the rate of the slow transition equalled the rate of ATP hydrolysis. Accordingly, the observed fluorescence change, scaled to the phosphate burst, was a weighted average of the signals of the tight binding and hydrolysis steps. The fast phase in the fluorescence transient and a corresponding lag in the phosphate burst make it appear as though the fluorescence rate were faster than hydrolysis. However, the phosphate data can be shown to superimpose on the slow phase of the fluorescence transient and the two processes occur at the same rate within the limits of error. We have therefore assigned the fast, 16% fluorescence transition to the tight ATP binding step and the slower, 20% increase to the ATP hydrolysis step (amplitudes refer to 20 °C, 0.1 M KCl).

Previous reports that the fluorescence rate was twice as fast as the rate of hydrolysis (Sleep & Taylor, 1976; Taylor, 1977) appear to be in error in part due to fitting the biphasic fluorescence trace to a single exponential and in part due to a temperature difference between the stop-flow and quench-flow instruments. Under the same conditions (50 mM KCl, pH 6.9) with somewhat closer temperature control (3.3 ± 0.5 °C), we now obtain a rate of 7 ± 1 s^{-1} for the rate of phosphate production and 7.9 ± 0.7 s^{-1} for the maximum fluorescence rate obtained by fitting to the slow phase (at 200 μM ATP).

Discussion

The steps in the SF-1 and acto-SF-1 ATPase mechanisms have been reinvestigated by measurements of the amplitude and rate of the fluorescence signal and the rates of the tight binding and hydrolysis of ATP. The amplitude of the SF-1 fluorescence signal decreased with increasing ATP concentrations; the time course showed a small deviation from a single exponential term; and the concentration dependence of the apparent rate constant deviated markedly from a hyperbola. These results require revision of the scheme originally proposed by Bagshaw & Trentham. In the Bagshaw–Trentham scheme, the fluorescence transient was attributed to a two-step rapid equilibrium mechanism with a rate-limiting tight ATP binding step. It was assumed that hydrolysis was much faster than the observed fluorescence rate and, therefore, the fluorescence change accompanying hydrolysis was kinetically unresolved. The present evidence is not compatible with this assignment of the rate constants.

Our data require the scheme to be revised as follows:

$$\mathrm{M} + \mathrm{ATP} \overset{1}{\rightleftharpoons} \mathrm{M{\cdot}ATP} \overset{2}{\rightleftharpoons} \mathrm{M{\cdot}ATP^*} \overset{3}{\rightleftharpoons} \mathrm{M{\cdot}Pr^{**}} \overset{\text{slow}}{\rightleftharpoons} \mathrm{M} + \mathrm{Pr} \quad (2)$$

The biphasic fluorescence transients and the nonhyperbolic dependence of the rate on ATP concentration require that two fluorescence changes contribute to the signal. The loss of signal amplitude at high ATP concentrations indicates that step 2 is fast compared with the dead time of the apparatus and is much faster than step 3 (hydrolysis). The maximum observable rate at high ATP concentration is thus the hydrolysis reaction.

This interpretation is strengthened by direct measurement of ATP binding and hydrolysis. At 10 °C and 10 mM KCl the rates of fluorescence enhancement and hydrolysis both reached a maximum rate of 20–25 s^{-1} and there was a loss of one-third of the fluorescence signal. Quenching with excess unlabeled ATP showed that ATP was irreversibly bound at a rate at least five times faster than the observed fluorescence signal. Moreover, the rate of irreversible binding corresponded approximately to the rate of the fast fluorescence signal. These observations support our assignment of $k_2 \gg k_3$ and identify the first fluorescence transition with tight ATP binding and the second transition with hydrolysis. In a preliminary report, Chock & Eisenberg (1977) have also described similar results, namely, tight ATP binding at a rate which exceeds both the rate of the observed fluorescence signal and the rate of phosphate production. They proposed that the hydrolysis step makes a "significant" contribution to the fluorescence signal, but they did not observe a fast fluorescence change associated with the binding step.

The inference that the initial collision complex is in rapid equilibrium with free ATP is based upon less direct evidence. A simpler two step scheme could account for the data: M + ATP $\rightleftharpoons$ M·ATP* $\rightleftharpoons$ M·Pr**. However, this scheme is less reasonable in that it requires an instantaneous fluorescence change and irreversible binding upon collision of ATP with the enzyme active site. In addition, the observed apparent second-order rate constant would define the rate of collision for this model and a value of 2×10^6 M^{-1} s^{-1} is considered to be much to small for a simple ligand binding process (Gutfreund, 1975). Although these arguments are not conclusive, it is most reasonable to require the formation of an initial collision complex, M·ATP, followed by a first-order transition to a state of enhanced fluorescence and tight ATP binding, M·ATP*.

The solution of the rate equation for the above mechanism (eq 2) is:

$$\mathrm{M{\cdot}ATP^*} = 1/(K_3 + 1) \times \left(1 + \frac{\bar{k}_3 - \lambda(K_3 + 1)}{(\lambda - \bar{k}_3)} \exp(-\lambda t) + \frac{\lambda \bar{k}_3}{(\lambda - \bar{k}_3)} \exp(-\bar{k}_3 t)\right)$$

$$\mathrm{M{\cdot}Pr^{**}} = K_3/(K_3 + 1) \times \left(1 + \frac{\bar{k}_3}{(\lambda - \bar{k}_3)} \exp(-\lambda t) - \frac{\lambda}{(\lambda - \bar{k}_3)} \exp(-\bar{k}_3 t)\right)$$

where $\lambda = K_1 k_2 [\mathrm{ATP}]/(K_1[\mathrm{ATP}] + 1)$ and $\bar{k}_3 = k_3 + k_{-3}$. The fluorescence signal is given by a weighted sum of the two states: F = 16 M·ATP* + 41 M·Pr**, such that the amplitude is 36 for a burst of 0.8.

The maximum rate of the fluorescence signal at very high ATP concentrations determines $\bar{k}_3$. Since λ approaches k_2 which is much larger than $\bar{k}_3$, the signal would be markedly biphasic at high ATP concentrations. However, the loss in signal amplitude requires k_2 to be 1500 to 2000 s^{-1} such that most of the fast phase is lost in the dead time of the stopped-flow instrument. The observable signal deviates only slightly from a single exponential term. The maximum rate at 20 °C, pH 7, 0.1 M KCl gives $\bar{k}_3 = 125 \pm 10$ s^{-1}. The size of the phosphate burst under these conditions was 0.8 (Taylor, 1977) which defines $K_3 \cong 4$ (see Bagshaw & Trentham, 1973); thus $k_3 = 100$ s^{-1} and $k_{-3} = 25$ s^{-1}.

At low ATP concentrations ($K_1[\mathrm{ATP}] \ll 1$), $\lambda \ll \bar{k}_3$ and the rate is approximately $K_1 k_2 [\mathrm{ATP}]$, with a small lag arising from $\bar{k}_3$. Thus the apparent second-order rate constant defines $K_1 k_2 = 2.5 \times 10^6$ M^{-1} s^{-1} at 20 °C, pH 7, 0.1 M KCl. If $k_2 = 2000$ s^{-1}, then K_1 is approximately 10^3 M^{-1} which is 5 to 10 times smaller than the value previously assigned to the initial association constant by fitting the rate data to a hyperbola.

The kinetic behavior of the above mechanism was compared with experimental results by calculating the time dependence of the fluorescence signal at various ATP concentrations and by fitting the calculated fluorescence transients to a single exponential. The calculated curves generated from this model using these parameters satisfactorily reproduced the experimental fluorescence signals over the entire range of ATP concentrations. There was a small lag at low ATP concentration and a fast phase at high ATP concentration. The apparent rate constant obtained by fitting the calculated curve to a single exponential deviated from a hyperbolic dependence on ATP concentration and the maximum rate decreased slightly at high ATP concentrations (see Figure 2). In addition, the fast phase led to a loss in signal amplitude in agreement with the data described in Figure 2 for an instrument dead time of 1.5 ms. The uncorrected amplitude at 500 μM ATP defines the amplitude of the second fluorescence transition to be 20% which leaves 16% for the first transition. Due to a lag in the formation of M·Pr**, there is virtually no signal loss attributable to step 3. Therefore, the corrected amplitude based upon the observed rate overestimates the amplitude of this step.

Experiments performed using SF-1 modified by iodoacetamide provided additional support for the mechanism (Sleep et al., 1978). Modification decreases the rate of both fluorescence transitions and decreases the amplitude of the second transition relative to the amplitude of the first. Thus, both fluorescence changes are easily observable and well separated in the transient. Under these conditions, the rate of phosphate production agreed with the rate of the slow fluorescence change and the rate of tight ATP binding was well correlated with the fast phase.

We note that another piece of evidence in favor of the

original Bagshaw–Trentham scheme was the similarity in the maximum observed rate of the fluorescence signals for ADP and ATP, suggesting that step 2 was measured since this conformation change might be similar for the binding of either nucleotide. This problem will be considered elsewhere but the agreement appears to be fortuitous since the rates for the two nucleotides show a different ionic strength dependence and the ADP signal also consists of two fluorescence transitions (Johnson et al., 1978).

As opposed to previous results (Bagshaw et al., 1974), our observations show that the maximum rate of the fluorescence signal for ATP binding increased with ionic strength, while the apparent second-order rate constant decreased (Figure 5); that is, k_3 increased while K_1k_2 decreased. Since ln K_1k_2 was linear in the square root of ionic strength corresponding to a charge product of approximately 2, the ionic strength dependence could arise largely from the binding of Mg ATP^{2-} to a site on the enzyme with a single positive charge. We note, however, that the Debye–Hückel theory rigorously applies only to uniformly charged spheres at very low ionic strength; thus, the charge product need not be quantitatively correct and may underestimate the actual value.

The reassignment of the fluorescence steps for SF-1 and the observation of a fluorescence enhancement on the association of acto-SF-1 eliminates the discrepancies in the mechanisms proposed for acto-SF-1 by Sleep & Taylor (1976) or Chock et al. (1976). It was shown by the former authors that the amplitude of fluorescence enhancement was essentially the same for SF-1 and acto-SF-1 at high ATP concentrations while Chock et al. obtained a value approximately 40% lower for acto-SF-1 as compared with SF-1 but at a lower ATP concentration. The source of the discrepancy is the signal loss for SF-1 compared to a constant amplitude obtained for acto-SF-1. It is evident in Figure 4 that the amplitude for acto-SF-1 is 40–50% smaller than for SF-1 in the ATP concentration range of 50–100 μM employed by Chock et al. but the amplitudes are approximately equal at high ATP concentrations.

The missing fluorescence in the acto-SF-1 reaction is accounted for by a 14% enhancement on formation of the acto-SF-1 complex. The origin of this enhancement is not known and the myosin in the AM state need not resemble the myosin in the M·ATP* state in any property other than the fluorescence emission. Moreover, the 14% enhancement of AM did not agree precisely with the 16% enhancement defined for the M·ATP* state, and it is not known whether this difference is real since a 2% change in the AM ⇀ M·ATP* reaction might not have been detected. Therefore it is not appropriate to label the actomyosin as AM*. The new state, postulated by Sleep & Taylor (M·ATP^+) is not required since it was introduced to explain the discrepancy with the original SF-1 mechanism of Bagshaw & Trentham. Similarly, the conclusion of Chock et al. (1976) that M·ATP* forms more rapidly when ATP binds to acto-SF-1 than when it binds to SF-1 is incorrect. The rates are identical within a factor of two.

The complete scheme which is consistent with the evidence is:

$$\begin{array}{ccccccc} & & & & & & \mathrm{AM + Pr} \\ & & & & & & k_5 \uparrow \\ \mathrm{AM + ATP} & \overset{K_1'}{\rightleftharpoons} & \mathrm{AM \cdot ATP} & \overset{k_2'}{\longrightarrow} & \mathrm{AM \cdot ATP^*} & & \mathrm{AM \cdot Pr^{**}} \\ & & & & \downarrow k_d & & \uparrow k_4 \\ \mathrm{M + ATP} & \overset{K_1}{\rightleftharpoons} & \mathrm{M \cdot ATP} & \overset{k_2}{\longrightarrow} & \mathrm{M \cdot ATP^*} & \underset{k_{-3}}{\overset{k_3}{\rightleftharpoons}} & \mathrm{M \cdot Pr^{**}} \end{array} \qquad (3)$$

The M·ATP* state is common to both pathways since the amplitude and rate of step 3 are the same for both SF-1 and acto-SF-1. Quenching experiments show that ATP is tightly bound to acto-SF-1 at a rate which is larger than the rates of the observed fluorescence or hydrolysis signals and the rate is roughly equal to the rate of dissociation. Thus a tightly bound ATP state precedes or accompanies the dissociation step and actomyosin dissociates to yield M·ATP* directly. By analogy with the myosin pathway, there may be two AM–ATP states with a conformation change preceding dissociation. It should be noted that k_2 (in the myosin scheme) is very large and if a similar transition occurs with acto-SF-1 it would be fast enough to account for the rate of dissociation; the maximum rate of dissociation can be either k_2' or k_d, whichever is slower. The apparent second-order rate constant defined by the partial reaction AM + ATP ⇀ AM·ATP → A + M·ATP* is approximately 4×10^6 M^{-1} s^{-1} (20 °C, 0.1 M KCl, pH 7) and the reaction as measured by the rate of dissociation exhibited ionic strength dependence similar to SF-1. In the case of slower actomyosins in which the maximum rate of dissociation has been measured, the concentration dependence is consistent with a rapid equilibrium with $K_1' = 10^3$ to 10^4 M^{-1} (Taylor & Marston, 1978). Thus K_1 is similar to K_1' and k_2 may be comparable to k_2'.

One might expect to observe an increase in fluorescence on formation of AM·ATP* followed by a decrease in fluorescence with dissociation in analogy to the myosin pathway. The absence of any detectable fluorescence change during or prior to dissociation is understandable because dissociation is sufficiently fast to maintain a very low concentration of AM·ATP* during the transient.

The association constant for the binding of M·ATP* to actin has to be much smaller than for the binding of M to actin to account for dissociation. Since K_1 and K_1' probably differ by a factor of 2 or less, the transition of AM·ATP to AM·ATP* must be responsible for dissociation and $K_2' \ll K_2$. From the studies of Mannherz et al. (1974) and Wolcott & Boyer (1975), K_2 is the order of 10^7 to 10^8. A value of K_2' of 10^3 to 10^4 would be sufficiently low to produce dissociation of AM·ATP*. The significance of the very strong binding of substrate to myosin is the requirement for a large interaction to lower the association constant of the actin in the ternary complex, AM·ATP*, while maintaining a reasonably high binding constant for the substrate to actomyosin.

The actomyosin pathway (eq 3) is the simplest scheme consistent with the evidence presented here and in a previous study of the recombination steps (White & Taylor, 1976). We do not rule out the possibility of additional myosin intermediate states. While step 3 is identified with hydrolysis because the same rate was obtained for the fluorescence and phosphate signals, the evidence could also be explained by an isomerization at rate k_3 followed by a much faster hydrolysis. An additional myosin-product intermediate (M·Pr^+) has been proposed (Chock et al., 1976) to account for the behavior at high actin concentrations. The current study does not provide evidence for or against the refractory state model and eq 3 can be made to agree with the scheme of Chock et al. by allowing transition 4 to occur in two steps.

Except for the addition of asterisks to distinguish states by fluorescence emission, the mechanism (eq 3) is essentially the same as proposed by Lymn & Taylor (1971) in that following actomyosin dissociation, hydrolysis occurs on the free myosin and actin recombines with a myosin–product state to complete the cycle.

Acknowledgments

We would like to thank Mrs. Aldona Rukuiza for excellent technical assistance and Dr. N. C. Yang of the Department

of Chemistry for the use of the fluorescence spectrophotometer.

References

Bagshaw, C. R., & Trentham, D. R. (1973) *Biochem. J. 133,* 323–328.
Bagshaw, C. R., & Trentham, D. R. (1974) *Biochem. J. 141,* 331–349.
Bagshaw, C. R., Eccleston, J. F., Eckstein, F., Goody, R. S., Gutfreund, H., & Trentham, D. R. (1974) *Biochem. J. 141,* 351–364.
Chock, S. P., & Eisenberg, E. (1974) *Proc. Natl. Acad. Sci., U.S.A. 71,* 4915–4919.
Chock, S. P., & Eisenberg, E. (1977) *Fed. Proc., Fed. Am. Soc. Exp. Biol. 36,* 830.
Chock, S. P., Chock, P. B., & Eisenberg, E. (1976) *Biochemistry 15,* 3244–3253.
Gutfreund, H. (1975) *Prog. Biophys. Mol. Biol. 29,* 161–195.
Hitchcock, S. (1973) *Biochemistry 12,* 2509–2515.
Johnson, K. A., Trybus, K. M., & Taylor, E. W. (1978) *Biophys. J. 21,* 44a.
Koretz, J. F., & Taylor, E. W. (1975) *J. Biol. Chem. 250,* 6344–6350.
Lowey, S., Slayter, M. S., Weeds, A. G., & Baker, H. (1969) *J. Mol. Biol. 42,* 1–29.
Lymn, R. W., & Taylor, E. W. (1970) *Biochemistry 9,* 2975–2983.
Lymn, R. W., & Taylor, E. W. (1971) *Biochemistry 10,* 4617–4624.
Mannherz, H. G., Schenck, H., & Goody, R. S. (1974) *Eur. J. Biochem. 48,* 287–295.
Margossian, S. S., Lowey, S., & Barshop, B. (1975) *Nature (London) 258,* 163–166.
Sleep, J. A., & Taylor, E. W. (1976) *Biochemistry 15,* 5813–5817.
Sleep, J. A., Trybus, K. M., Johnson, K. A., & Taylor, E. W. (1978) *J. Mechanochem. Cell Motil.* (in press).
Spudich, J. A., & Watt, S. (1971) *J. Biol. Chem. 246,* 4866.
Starr, R., & Offer, G. (1971) *FEBS Lett. 15,* 40–44.
Taylor, E. W. (1977) *Biochemistry 16,* 732–740.
Taylor, E. W., & Marston, S. A. (1977) *Fed. Proc., Fed. Am. Soc. Exp. Biol. 36,* 830.
Taylor, E. W., Lymn, R. W., & Moll, G. (1970) *Biochemistry 9,* 2984.
Weeds, A. G., & Pope, B. (1976) *J. Mol. Biol. 111,* 129–157.
Weeds, A. G., & Taylor, R. S. (1975) *Nature (London) 257,* 54–56.
Werber, M., Szent-Gyorgyi, A. G., & Fasman, G. (1972) *Biochemistry 11,* 2872–2883.
White, H. D., & Taylor, E. W. (1976) *Biochemistry 15,* 5818–5826.
Wolcott, R. G., & Boyer, P. D. (1974) *Biochem. Biophys. Res. Commun. 57,* 709–716.

Physicochemical Characterization and Molecular Organization of the Collagen A and B Chains†

R. Kent Rhodes and Edward J. Miller*

ABSTRACT: Collagen containing the A and B chains has been isolated and purified from pepsin digests of human placenta, bone, and cartilage using convenient procedures which allow maximum recovery of the collagen in highly purified form. In addition, phosphocellulose chromatography has been employed to achieve complete resolution of the A and B chains following denaturation of the collagen. Utilizing these procedures, it has been observed that the stoichiometry of the A and B chains in collagen prepared from the different tissues is quite variable. The chain ratios for A and B chains in the collagen derived from placenta and bone are 1:1 and 1:1.6, respectively. On the other hand, the collagen derived from cartilage lacks the A chain but contains significant quantities of B chain. Molecular weight estimates for the chains, as determined by agarose molecular sieve chromatography and sodium dodecyl sulfate–polyacrylamide gel electrophoresis, indicate that the B chain is approximately 10% larger than the A chain. Thermal denaturation studies on collagen containing the A and B chains from placenta indicate that the melting transition is characterized by two distinct phases. Examination of the collagen denatured during the initial phase showed that it was comprised largely of A chains, whereas the collagen remaining in native conformation at this time was comprised largely of B chains. It is concluded from these data that the A and B chains exist in separate molecular species with the chain compositions $[A]_3$ and $[B]_3$ being the most likely and most prevalent forms.

Information on the genetic diversity of mammalian collagens has recently been extended by reports from this laboratory (Chung et al., 1976) and others (Burgeson et al., 1976) of new collagenous components. Preliminary characterization of the new chains, provisionally designated as the A and B chains, showed that each chain was approximately the size of α components derived from interstitial collagens. Nevertheless, the new chains differed markedly with respect to compositional features from the constituent chains of the known interstitial collagens. Moreover, though significant differences between the two chains exist, they both resemble chains derived from isolated basement membranes in their amino acid content. Such features include the presence of relatively large amounts

† From the Institute of Dental Research and Department of Biochemistry, University of Alabama in Birmingham, Birmingham, Alabama 35294. *Received March 22, 1978.* Supported by United States Public Health Service Grants HL-11310 and DE-02670.

0006-2960/78/0417-3442$01.00/0